RSC Advances

PAPER

View Article Online
View Journal | View Issue

Cite this: *RSC Adv.*, 2017, **7**, 44082

Cascade catalytic hydrogenation–cyclization of methyl levulinate to form γ-valerolactone over Ru nanoparticles supported on a sulfonic acid-functionalized UiO-66 catalyst†

Zhenzhen Lin, Xiaoxiong Cai, Yanghe Fu, Weidong Zhu and Fumin Zhang *

We herein report a high-yielding one-pot upgrade strategy for converting biomass-derived methyl levulinate (ML) into γ-valerolactone (GVL) over a dual-functional catalyst prepared by depositing Ru nanoparticles on a sulfonic acid-functionalized Zr-based metal–organic framework (SO_3H-UiO-66). Under the mild conditions of 80 °C and 0.5 MPa H_2 for 4 h in aqueous solution, a quantitative (100%) yield of GVL was obtained over the prepared Ru/SO_3H-UiO-66 catalyst. In contrast, a very limited yield of GVL was achieved in the control experiment by first hydrogenating the reactant ML over a metal catalyst without any acidity (*e.g.* Ru/C) to produce the 4-hydroxypentanoic acid methyl ester (4-HPME) intermediate, followed by treatment of this intermediate over the acidic SO_3H-UiO-66 support in the absence of metal. We also found that the catalytic activity and selectivity of Ru/SO_3H-UiO-66 were significantly suppressed upon neutralization of its acidic sites, thereby confirming the indispensable role of the sulfonic acid groups in promoting the intramolecular dealcoholation of the 4-HPME intermediate. Furthermore, the Ru/SO_3H-UiO-66 catalyst was recyclable over five cycles without any significant loss in its catalytic activity, thus rendering this precious metal/acid dual-functional catalyst a potential candidate for efficient GVL production under mild conditions.

Received 6th June 2017
Accepted 7th September 2017

DOI: 10.1039/c7ra06293a

rsc.li/rsc-advances

Introduction

To reduce the current dependence on fossil fuel resources and the associated environmental issues, the investigation of alternative effective routes to produce fuels and value-added chemicals from sustainable resources continues to receive growing attention.[1,2] In this context, biomass, an inexpensive, renewable, and widely available resource, has been recognized as a promising alternative to replace fossil fuel resources for the sustainable production of biochemicals and biofuels.[3,4] Among the various chemicals synthesized from biomass to date, γ-valerolactone (GVL) has been identified as an important molecule for use as a fuel additive, a food ingredient, a renewable solvent, and an ideal intermediate for production of alkenes and other valuable chemicals due to its benign properties and versatility.[5–9] In addition, the upgrade of GVL to a liquid hydrocarbon fuel has also been reported, with Dumesic and coworkers designing a system that integrates the conversion of GVL to butene *via* decarboxylation over a silica/alumina catalyst with the subsequent oligomerization of butene over an acidic catalyst (HZSM-5 or Amberlyst 70).[10] Indeed, they reported that the products contained mainly C_8, C_{12}, and C_{16} olefins, which are the key components present in gasoline and jet fuels. Furthermore, Serrano-Ruiz *et al.* studied the conversion of GVL over a dual-functional heterogeneous Pd/Nb_2O_5 catalyst to yield pentanoic acid and 5-nonanone,[11] which can be further converted into hydrocarbon fuels *via* hydrodeoxygenation.

To date, GVL has mainly been obtained from levulinic acid (LA), a platform molecule derived from lignocellulosic biomass, *via* a two-step catalytic process involving selective hydrogenation under a high pressure of H_2 and subsequent intramolecular dehydration.[5–9] Indeed, many reports exist into the catalytic conversion of LA using both homogeneous and heterogeneous noble and non-noble metal catalysts in liquid and vapor phase systems.[5–9,11–18] Among the various metals investigated, ruthenium appears to be the most active and selective metal for the conversion of LA to GVL, mainly due to its selective hydrogenation of carbonyl groups without altering other unsaturated functionalities.[11–18] However, traditional catalysts, such as commercial Ru/C, often exhibit leaching of the ruthenium species through the formation of metal–carboxylate complexes with LA, which is likely caused by the weak acidity of LA ($pK_a = 4.59$),[19–21] results in a low catalytic activity and poor catalyst reusability.

As an alternative substrate, levulinic ester, which is produced by the acid-catalyzed alcoholysis of various carbohydrate

Key Laboratory of the Ministry of Education for Advanced Catalysis Materials, Institute of Advanced Fluorine-Containing Materials, Zhejiang Normal University, 321004 Jinhua, People's Republic of China. E-mail: zhangfumin@zjnu.edu.cn

† Electronic supplementary information (ESI) available. See DOI: 10.1039/c7ra06293a

fractions of lignocellulose, is acid-free, and can also be converted to GVL.[5–9] Recently, several strategies based on the use of heterogeneous catalysts have been reported for the liquid-phase upgrade of methyl levulinate (ML) to GVL.[22–24] For example, Hengne and co-workers reported that a 5 wt% Ru/C catalyst was active in the hydrogenation of ML, giving a conversion of 95% and a GVL selectivity of 91% under a H_2 pressure of 3.4 MPa at 130 °C over 2 h in methanol.[22] In addition, Nadgeri *et al.* reported that a 100% conversion of ML with 32% GVL selectivity could be achieved over a 1.0 wt% Ru/graphite catalyst under 3 MPa of H_2 at 70 °C over 10 min in water.[23] However, no apparent increase in the GVL yield was observed when the reaction time was extended further to 4 h. Generally, the conversion of ML to GVL involves a two-step reaction sequence, namely hydrogenation of the carbonyl groups over metal sites to give the 4-hydroxypentanoic acid methyl ester (4-HPME) intermediate, and subsequent dealcoholization of 4-HPME to yield GVL catalyzed by the acidic sites (Scheme 1). Therefore, the prerequisite for establishing an efficient ML to GVL conversion process is to develop high performance dual-functional solid catalysts containing metal nanoparticles and acidic sites to enhance the process efficiency (*i.e.*, catalytic activity and selectivity) and process simplicity.[14,15]

As a relative new class of crystalline ordered materials, metal–organic frameworks (MOFs), have attached significant attention in several areas, in particular in the field of catalysis, because of their controllable pores characteristics, large internal surface areas, and tunable chemical properties.[25–27] For example, the typical Zr-based MOF, UiO-66, is comprised of 12-coordinated $Zr_6O_4(OH)_4$ clusters that are connected three-dimensionally with terephthalic acid (BDC) linkers.[28–30] In this case, the cavities present in the UiO-66 structure provide the possibility to encapsulate metal nanoparticles within its frameworks to ultimately prevent nanoparticles agglomeration.[31–33] Moreover, the BDC linker of UiO-66 can be tuned to introduce functionality by partially or integrally replacing it with analogous organic linkers *via* direct or post-modification.[35,36] In combination with its high thermal and chemical stabilities, the above properties render UiO-66 an ideal candidate for application in heterogeneous catalysis.[31–39]

Thus, we herein report the catalytic cascade hydrogenation–cyclization of ML with the aim of producing GVL in high-yields over Ru nanoparticles supported on a functionalized UiO-66 catalyst. Through the appropriate tuning of the molar ratio of the mixed organic linkers of 2-sulfonylterephthalic acid monosodium salt (2-$NaSO_3$-H_2BDC) and BDC, we expect that a highly stable sulfonic acid-functionalized UiO-66 (SO_3H-UiO-66) catalyst can be synthesized easily *via* a direct solvothermal approach.[40] Subsequently, Ru nanoparticles will be introduced into the cavities of SO_3H-UiO-66 using a wet impregnation technique and the resulting Ru/SO_3H-UiO-66 catalyst will be employed in the aqueous-phase conversion of ML to GVL. We expect that the SO_3H-UiO-66 frameworks will distribute homogeneously in the aqueous medium due to their hydrophilic properties and low density,[41] thereby facilitating the adsorption/diffusion of the reactants. Furthermore, the abundant cavities present in the SO_3H-UiO-66 host will be expected to allow the facile dispersal and stabilization of the imbedded Ru nanoparticles, which can then adsorb and activate H_2 and promote the hydrogenation of ML to yield 4-HPME. Finally, we propose that the acidic –SO_3H groups tethered on the MOF frameworks will accelerate the subsequent intramolecular dealcoholization of 4-HPME to afford GVL in high yields. In this context, our aim is to construct a multifunctional catalyst coupled with precious metal nanoparticles and acidic sites in a single support to enhance catalytic activity and give a reproducible performance in the upgrade of ML.

Experimental

Catalyst preparation

The parent SO_3H-UiO-66 support was synthesized using a solvothermal method according to the procedure reported by Foo *et al.*[40] with slight modification. Detailed information regarding the materials and methods employed can be found in the ESI.†

For preparation of the 5.0 wt% Ru/SO_3H-UiO-66 catalyst, a sample the pre-dried SO_3H-UiO-66 (0.2 g) was dispersed in deionized water (20 mL) at 25 °C. An aqueous $RuCl_3$ solution (2.08 mL, 0.05 mol L^{-1}) was then added to the above suspension under vigorous stirring and the resulting slurry was stirred at 25 °C for 24 h. Subsequently, the reduction of Ru^{3+} was conducted by the dropwise addition of aqueous $NaBH_4$ (3.6 mL, 28 mg; $[NaBH_4]/[Ru] = 7$) into the above suspension upon cooling using an ice-bath. After allowing the reduction to proceed for 30 min, the resulting solid was collected by centrifugation prior to treatment in a solution of diluted HCl (3.6 mL, 0.2 mol L^{-1}) in methanol, and rinsed with methanol and water to remove any excess additional HCl. Finally, the obtained solid was dried overnight at 120 °C under reduced pressure prior to use. For comparison, the Ru nanoparticles supported on UiO-66 and NH_2-UiO-66 (referred to as 5.0 wt% Ru/UiO-66 and 5.0 wt% Ru/NH_2-UiO-66, respectively) were also prepared using above method with BDC and NH_2-BDC as the starting organic ligand.

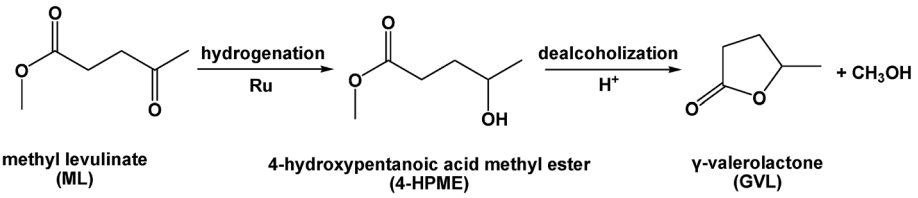

Scheme 1 Conversion of ML to GVL *via* hydrogenation followed by intramolecular dealcoholization.

Catalytic hydrogenation–cyclization of ML

The catalytic hydrogenation–cyclization of ML was performed in a 50 mL Teflon-lined autoclave reactor equipped with a sample port and a magnetic stirrer. In a typical reaction, ML (0.5 g), catalyst (0.05 g), and H_2O (15 mL) were introduced into the autoclave and purged five times with H_2 at room temperature. The autoclave was then heated to 80 °C and pressurized with H_2 to 0.5 MPa. After initiating agitation at 980 rpm, a steady pressure was maintained throughout the reaction. Samples of the reaction mixture (0.3 mL) were withdrawn at allocated reaction times and the catalyst was removed by centrifugation prior to analysis the reaction mixture by gas chromatography (GC, GC-2014, Shimadzu, equipped with an FID detector and a capillary column, DB-5, 30 m × 0.32 mm × 0.25 μm). To determine the catalyst reusability, the used catalyst was recovered by centrifugation, washed with ethanol, and dried in a vacuum desiccator at 150 °C for 5 h prior to its application in the subsequent reaction cycle.

Results and discussion

We initially examined and compared the physical properties of the prepared catalysts. As indicated in the powder X-ray diffraction (XRD) patterns shown in Fig. 1A, no loss of crystallinity was observed for the Ru/SO_3H-UiO-66 catalyst compared to the parent SO_3H-UiO-66 support, suggesting that the integrity of the SO_3H-UiO-66 framework was maintained following Ru immobilization by the simple wetness impregnation method employed herein.[42] In addition, no diffraction peaks associated with any Ru species were observed, likely due to the low Ru content and/or the small Ru nanoparticle size in the Ru/SO_3H-UiO-66 structure.[31–34] Furthermore, a significant decrease in both the pore volume and the quantity N_2 adsorbed was observed for Ru/SO_3H-UiO-66 with respect to the pristine SO_3H-UiO-66, indicating that the cavities of SO_3H-UiO-66 were partially occupied by the dispersed Ru nanoparticles (Fig. 1B and S1 in the ESI†). Moreover, the presence of sulfonic acid groups tethered on the UiO-66 frameworks were confirmed by Fourier transform infrared (FTIR) spectroscopy. In this case, the absorption bands at 1250 cm^{-1} and 1020 cm^{-1} were assigned to the symmetric stretching vibration of O═S═O and the stretching mode of S═O, respectively, while the band at 1078 cm^{-1} was assigned to the n-plane skeletal vibration of the benzene rings substituted by a sulfonic acid group (Fig. 1C).[40] Interestingly, no peak shift was observed following loading the Ru nanoparticles onto the support, thereby indicating that the –SO_3H groups are present as "free" sulfonic acid groups in the supported catalyst.[43] Thermogravimetric analysis (TGA) curves also confirmed the integrity of the SO_3H-UiO-66 frameworks following introduction of the Ru nanoparticles, with the thermal stability up to 450 °C being maintained throughout the synthesis and functionalization procedures (Fig. 1D).

Analysis of the various samples by inductively coupled plasma atomic emission spectroscopy (ICP-AES) indicated that the measured Ru loadings were close to the nominal amounts present in the precursor (Table S1 in ESI†). In addition, no sodium ions were detected, indicating that all the Na^+ ions of the 2-$NaSO_3$-H_2BDC ligand had been exchanged with H^+ (from HCl) during preparation. In addition, as shown in the sulfur X-ray photoelectron spectrum (XPS) in Fig. 2A, a single S 2p peak attributable to the sulfonic acid groups was present at 168.3 eV,[43] which indicated that almost all S was present in the

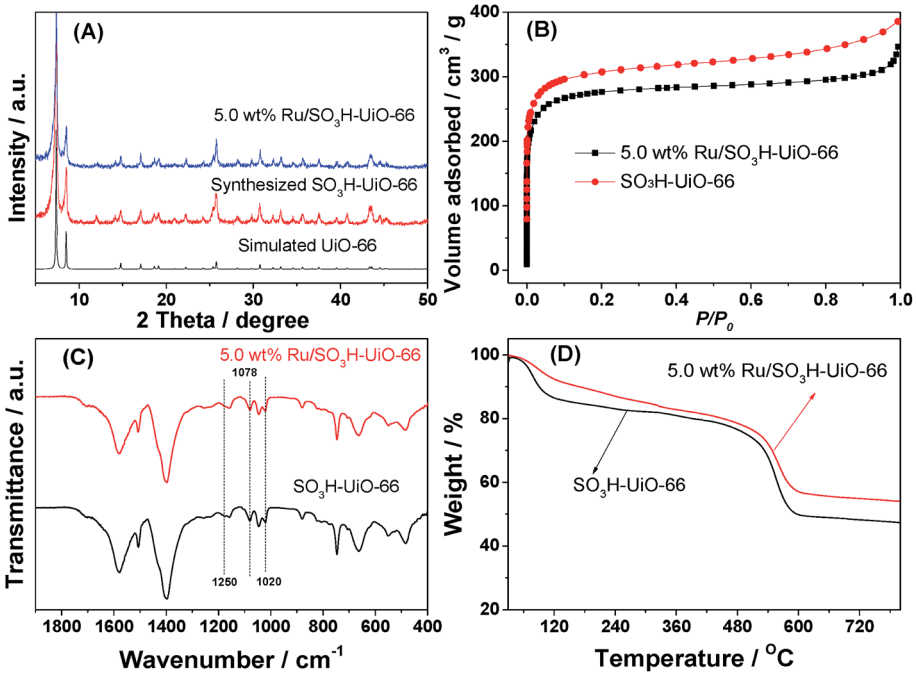

Fig. 1 (A) XRD patterns, (B) N_2 adsorption isotherms, (C) FTIR spectra and (D) TGA curves of the SO_3H-UiO-66 support and the prepared Ru/SO_3H-UiO-66 catalyst.

forms of sulfonic acid, thereby confirming the FTIR observations. Furthermore, the presence of Ru^0 in the catalyst was confirmed by XPS analysis (Fig. 2B), as clearly demonstrated by the presence of a band at 461.8 eV, which is characteristic of the zerovalent Ru species.[16,43] Moreover, acid–base titrations indicated that the acidity of Ru/SO_3H-UiO-66 was 0.35 mmol g^{-1}.[36,44–46] It should be considered here that the missing-linker defect sites (consisting of Zr–OH sites) in SO_3H-UiO-66 also contributed to the total Brønsted acid content, although their acidity strength is significantly weaker than that of the –SO_3H sites.[28,36] We could therefore conclude that the quantified acidity originated primarily from the Brønsted acidity –SO_3H groups tethered on the UiO-66 frameworks.

Furthermore, energy-dispersive X-ray spectroscopy (EDX) mapping confirmed that the Ru nanoparticles were evenly distributed within SO_3H-UiO-66 (Fig. 3), while transmission electron microscopy (TEM) observations (Fig. 4) confirmed the uniformity of the 2–4 nm diameter Ru nanoparticles that were homogeneously dispersed within the SO_3H-UiO-66 matrix. A characteristic interlayer spacing of 0.23 nm was also determined from the high-resolution TEM image (Fig. 4B), which was ascribed to the (100) plane of the hcp-structured Ru nanoparticles.

Following successful characterization, the 5.0 wt% Ru/SO_3H-UiO-66 catalyst was tested in the aqueous-phase conversion of biomass-derived ML to GVL in an autoclave at 80 °C and at a hydrogen pressure of 0.5 MPa (Fig. 5). In the absence of catalyst or in the presence of only pristine SO_3H-UiO-66, no reaction took place. However, upon the addition of 5.0 wt% Ru/SO_3H-UiO-66 to the reaction system, the concentration of 4-HPME increased dramatically within the first 60 min, accompanied by a sharp decrease in the ML concentration, thereby demonstrating that ML is mainly hydrogenated to yield 4-HPME in the initial step. Interestingly, the production of GVL was also observed in the initial 5 min of the reaction, implying that either intramolecular dealcoholation of 4-HPME occurred immediately, or that ML could be converted directly into GVL.[22–24] As the reaction progressed, the intramolecular dealcoholation of 4-HPME continued smoothly, with almost complete conversion of 4-HPME to GVL being observed after 400 min. Remarkably, GVL was found to be stable in the aqueous reaction system, as increasing the reaction time further to 540 min did not generate any additional hydrogenation or hydrogenolysis products.

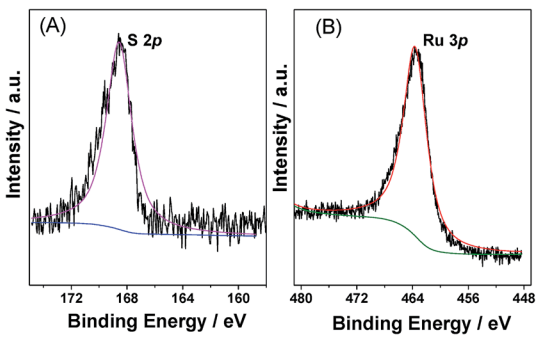

Fig. 2 XPS spectra of (A) S spectrum and (B) Ru 3p for the prepared 5.0 wt% Ru/SO_3H-UiO-66 catalyst.

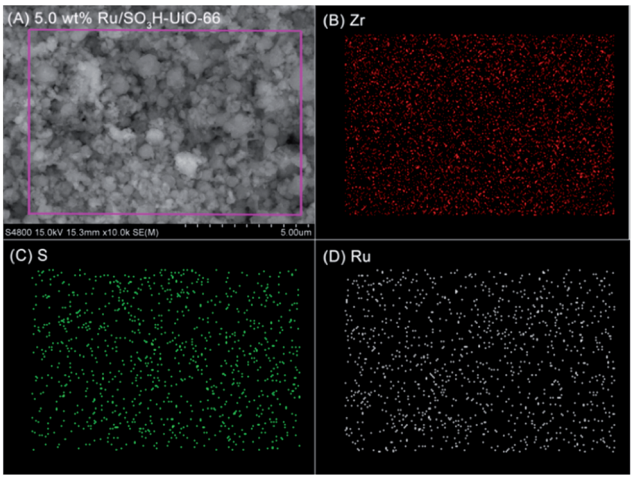

Fig. 3 SEM and EDS analyses of the 5.0 wt% Ru/SO_3H-UiO-66 catalyst.

Interestingly, the one-pot conversion of ML into GVL over heterogeneous catalysts has been reported previously (see Table 1).[23,24,47] For example, the use of a commercially available 5.0 wt% Ru/C in methanol gave an ML consumption of 97.8% over 160 min at 130 °C and 1.2 MPa H_2 with 89.4% selectivity towards GVL (Table 1, entry 1).[47] Indeed, the use of alcohols as the reaction medium for levulinic ester hydrogenation appears advantageous, as such solvents can be derived from lignocellulosic biomass and so have a low environmental impact.[5–9] However, from the viewpoint of sustainable chemistry, the use of water as reaction medium is more desirable, since it is environmentally benign. We therefore attempted the conversion using water as the reaction solvent, and were surprised to find that superior results were obtained. More specifically, using the 5.0 wt% Ru/SO_3H-UiO-66 catalyst, a 74.5% yield of GVL was obtained under relatively mild reaction conditions (entry 4), which was a higher conversion than that obtained over a 4.5 wt% Ru/Zr_5SMS catalyst (entry 3).[23] Moreover, upon comparison of our 5.0 wt% Ru/SO_3H-UiO-66 catalyst with Ru/C and with the UiO-66- and NH_2-UiO-66- supported Ru nanoparticles (entries 5–8), it was apparent the Ru/SO_3H-UiO-66 catalyst gave a significantly higher ML conversion and GVL selectivity than the Ru/C. In contrast, Ru/UiO-66 and Ru/NH_2-UiO-66 exhibited only moderate activities, producing GVL in lower yields than Ru/SO_3H-UiO-66 (see Table S1 and Fig. S2–S6, ESI† for characterization of the control catalysts). Of course, it should be admitted that the metal dispersions may be different in the above different cases, which could also affect the reactivity. These results therefore suggest that the nature of the support plays a key role in determining the activity and selectivity of the Ru nanoparticles for the hydrogenation–cyclization of ML. Furthermore, it has been reported that the SO_3H-UiO-66-based catalyst is easily dispersed in water,[44] thereby enhancing contact between the catalyst and the substrate, and increasing the catalytic performance of Ru/SO_3H-UiO-66.

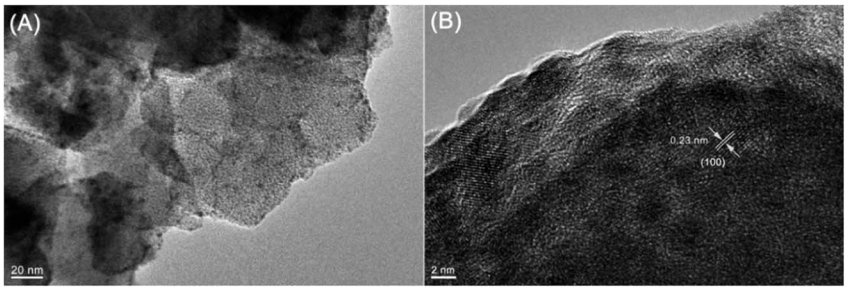

Fig. 4 (A) TEM image and (B) high-resolution image of the prepared 5.0 wt% Ru/SO_3H-UiO-66 catalyst.

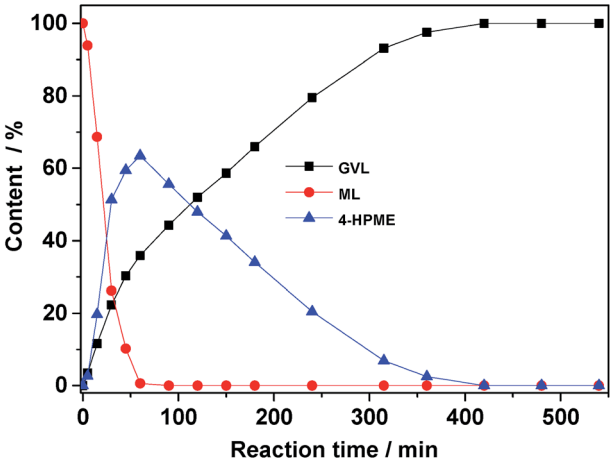

Fig. 5 Evolution of reactant and product distributions as a function of reaction time. Reaction conditions: ML (0.5 g), catalyst (0.05 g), H_2O (15 mL), 80 °C, 0.5 MPa H_2.

It was also expected that the acidic properties of the catalyst may play a key role in this reaction, and so we examined the pH of the reaction system in the presence of the 5.0 wt% Ru/SO_3H-UiO-66 catalyst, and found that it ranged from 4.8 to 5.1. As discussed above, the acidic sites of SO_3H-UiO-66 originate mainly from the sulfonic acid groups tethered to the UiO-66 frameworks. Thus, the high catalytic activity and selectivity of Ru/SO_3H-UiO-66 in this cascade reaction are likely due to the synergistic effects between the "host" and the "guest", where the Ru nanoparticles guests provide the H_2 activation/hydrogenation activity and the SO_3H-UiO-66 host offers the acidity, thereby triggering the subsequent intramolecular dealcoholation.[22–24]

To further explore the influence of the acid sites present in SO_3H-UiO-66 on the ML conversion, a control hydrogenation–cyclization experiment was performed over the 5.0 wt% Ru/SO_3H-UiO-66 catalyst and in the presence of a calculated amount of NaOH with respect to the acidic sites available on the catalyst (Fig. 6). As indicated, upon neutralization of the acidic sites by NaOH, the activity and selectivity of the catalyst decreased significantly, thereby confirming poisoning/neutralization of the acidic sites through the strong interaction with NaOH.[44] This result clearly demonstrates the importance of acidic sites in the catalytic intramolecular dealcoholation reaction.

In addition, another control experiment was conducted in order to clarify the possible reaction mechanism. As shown in the case (a) of Fig. 7, a small portion of GVL was formed over 5.0 wt% Ru/C along with the major HPME product by the catalytic hydrogenation reaction. Subsequently, we treated this intermediate with the SO_3H/UiO-66 support (0.05 g) at 70 °C upon removal of Ru/C by hot filtration. It was observed that the generated HPME was partially converted into GVL in the following 4 h (in the case (b) of Fig. 7), while the concentration of ML in this intermediate had no any change. These results consistently confirmed the importance of acidic sites in the catalytic intramolecular dealcoholation reaction. In our opinion, the formation of the small amount GVL in the presence of 5.0 wt% Ru/C could be probably ascribed to the following two reasons: HPME might be self-catalyzed to yield

Table 1 Comparison of the conversions and selectivities for the cascade catalytic hydrogenation–cyclization of ML using a range of catalysts

Entry	Catalyst	s/c^a	Solvent	Temp. (°C)	$p_{H_2}{}^b$ (MPa)	t (min)	Con.^{c} (%)	Sel.^{d} (%)
1	5.0 wt% Ru/C[47]	348	CH_3OH	130	1.2	160	97.8	89.4
2	5.0 wt% Ru/C[23]	118	CH_3OH	130	3.5	120	95	91
3	4.5 wt% Ru/Zr_5SMS[24]	199	CH_3OH	70	0.5	240	>99.9	67.1
4	5.0 wt% Ru/SO_3H-UiO-66	200	H_2O	70	0.5	240	>99.9	74.5
5	5.0 wt% Ru/SO_3H-UiO-66	200	H_2O	70	0.5	45	95.5	20.7
6	5.0 wt% Ru/UiO-66	200	H_2O	70	0.5	45	90.3	13.8
7	5.0 wt% Ru/NH_2-UiO-66	200	H_2O	70	0.5	45	73.7	14.6
8	5.0 wt% Ru/C	155	H_2O	70	0.5	45	44.6	10.3

[a] Molar ratio of ML to Pd in the catalyst used. [b] H_2 pressure. [c] Conversion of ML. [d] Selectivity for GVL.

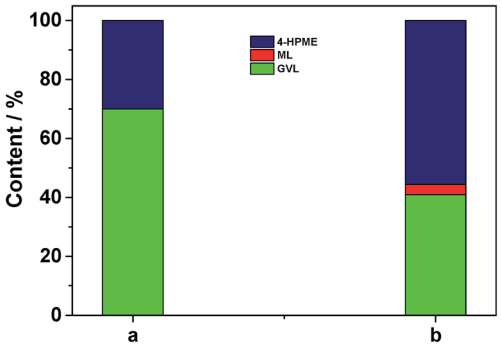

Fig. 6 Cascade catalytic hydrogenation–cyclization of ML over 5.0 wt% Ru/SO_3H-UiO-66 in (a) the absence and (b) the presence of 0.02 mmol NaOH. Reaction conditions: ML (0.5 g), catalyst (0.05 g), H_2O (15 mL), 80 °C, 0.5 MPa H_2 pressure, 30 min.

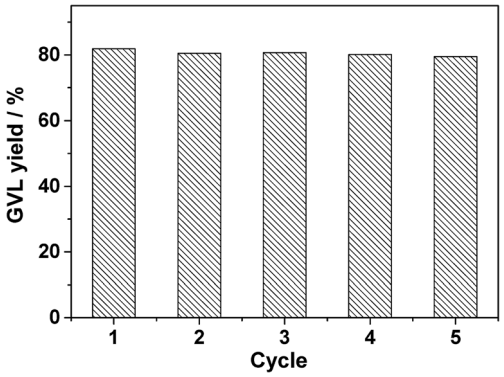

Fig. 8 Catalyst (5.0 wt% Ru/SO_3H-UiO-66) recyclability in the cascade catalytic hydrogenation–cyclization of ML. Reaction conditions: ML (0.5 g), catalyst (0.05 g), H_2O (15 mL), 80 °C, 0.5 MPa H_2 pressure, 240 min.

GVL under the reaction conditions; Ru clusters with a diameter size smaller than 1 nm (even single ruthenium site), which could not be observed by our conventional TEM or HRTEM techniques, were partially responsible for the direct conversion of ML to GVL. In the further work, we will investigate these factors in detail. Nevertheless, based on the above discussion, we can deduce that the mechanism to produce GVL from HPME apparently requires the Ru/SO_3H-UiO-66 rather than just the SO_3H-UiO-66 support. The metal–acid interfacial sites of the developed Ru/SO_3H-UiO-66 may be relevant to this transformation.

To allow the catalyst to be recycled, isolation from the reaction solution by facile filtration is preferable. In this case, filtration and washing of the spent 5.0 wt% Ru/SO_3H-UiO-66 catalyst allowed it to be recycled five times without any significant loss in catalytic activity (Fig. 8). Notably, XRD, N_2 adsorption, FTIR, EDX mapping, and ICP-AES measurements (Fig. S7–S10, ESI†) confirmed that the reused catalyst exhibited a comparable porous structure, Ru nanoparticle dispersion, and chemical composition as the fresh one. These results demonstrate that the prepared 5.0 wt% Ru/SO_3H-UiO-66 catalyst is sufficiently stable to be employed in the hydrogenation–cyclization of ML to yield GVL.

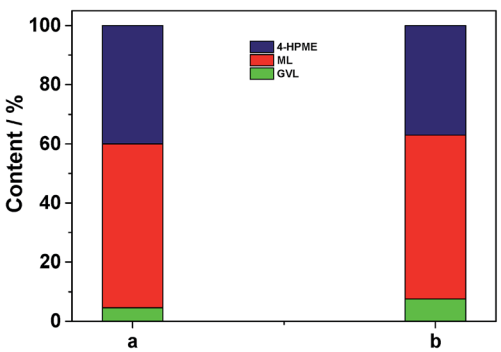

Fig. 7 Catalytic hydrogenation–cyclization of ML over 5.0 wt% Ru/C at 70 °C for 45 min (a) and treated the above filtrate in the presence of SO_3H-UiO-66 (0.05 g) at 70 °C for 4 h after removal of 5.0 wt% Ru/C by hot filtration (b). Other reaction parameters in the case (a) ML (0.5 g), 5.0 wt% Ru/C (0.05 g), H_2O (15 mL) and 0.5 MPa H_2 pressure.

Conclusions

In summary, we successfully developed a dual-functional Ru/SO_3H-UiO-66 catalyst for the high-yielding one-pot synthesis of γ-valerolactone from biomass-derived methyl levulinate under ambient conditions in water by loading ruthenium nanoparticles onto a highly stable sulfonic acid-functionalized Zr-based metal–organic framework (*i.e.*, SO_3H-UiO-66). This catalyst exhibited a high catalytic activity, high selectivity, and good reproducibility over five catalytic cycles. The excellent catalytic properties of Ru/SO_3H-UiO-66 were mainly ascribed to the synergistic catalytic effect of the imbedded tiny Ru nanoparticles and the Brønsted acidic sites of the SO_3H-UiO-66 support. Perhaps the metal–acid interfacial sites were responsible for this efficient transformation. We therefore expect that the developed 5.0 wt% Ru/SO_3H-UiO-66 catalyst will open a novel route to biomass upgrade involving metal/acid dual-functional synergistic catalysts in an environmentally benign solvent.

Conflicts of interest

There are no conflicts to declare.

Acknowledgements

This work was financially supported by National Natural Science Foundation of China (21576243), Public Project of Zhejiang Province of China (2016C37057), and New Talent Project for Undergraduates in Zhejiang Province (2017R404067).

References

1 J. C. Serrano-Ruiz, R. Luque and A. Sepulveda-Escribano, *Chem. Soc. Rev.*, 2011, **40**, 5266–5281.

2 M. J. Climent, A. Corma and S. Iborra, *Green Chem.*, 2014, **16**, 516–547.
3 K. Yan, Y. Yang, J. Chai and Y. Lu, *Appl. Catal., B*, 2015, **179**, 292–304.
4 C. B. Chen, M. Y. Chen, B. Zada, Y. J. Ma, L. Yan, Q. Xu, W. Z. Li, Q. X. Guo and Y. Fu, *RSC Adv.*, 2016, **6**, 112477–112485.
5 J. M. Tukacs, M. Bohus, G. Dibo and L. T. Mika, *RSC Adv.*, 2017, **7**, 3331–3335.
6 F. Liguori, C. Moreno-Marrodan and P. Barbaro, *ACS Catal.*, 2015, **5**, 1882–1894.
7 W. R. Wright and R. Palkovits, *ChemSusChem*, 2012, **5**, 1657–1667.
8 K. Hengst, M. Schubert, H. W. P. Carvalho, C. Lu, W. Kleist and J. D. Grunwaldt, *Appl. Catal., A*, 2015, **502**, 18–26.
9 F. D. Pileidis and M. M. Titirici, *ChemSusChem*, 2016, **9**, 562–582.
10 J. Q. Bond, D. M. Alonso, D. Wang, R. M. West and J. A. Dumesic, *Science*, 2010, **327**, 1110–1114.
11 J. C. Serrano-Ruiz, D. Wang and J. A. Dumesic, *Green Chem.*, 2010, **12**, 574–577.
12 Z. H. Zhang, *ChemSusChem*, 2016, **9**, 156–171.
13 C. Moreno-Marrodan and P. Barbaro, *Green Chem.*, 2014, **16**, 3434–3438.
14 S. Xu, D. Yu, T. Ye and P. Tian, *RSC Adv.*, 2017, **7**, 1026–1031.
15 Y. Wang, Z. Rong, Y. Wang, T. Wang, Q. Du, Y. Wang and J. Qu, *ACS Sustainable Chem. Eng.*, 2016, **5**, 1538–1548.
16 C. Xiao, T. W. Goh, Z. Qi, S. Goes, K. Brashler, C. Perez and W. Huang, *ACS Catal.*, 2016, **6**, 593–599.
17 Z. Wei, J. Lou, C. Su, D. Guo, Y. Liu and S. Deng, *ChemSusChem*, 2017, **10**, 1720–1732.
18 A. Villa, M. Schiavoni, C. E. Chan-Thaw, P. F. Fulvio, R. T. Mayes, S. Dai, K. L. More, G. M. Veith and L. Prati, *ChemSusChem*, 2015, **8**, 2520–2528.
19 P. P. Upare, J. M. Lee, D. W. Hwang, S. B. Halligudi, Y. K. Hwang and J. S. Chang, *J. Ind. Eng. Chem.*, 2011, **17**, 287–292.
20 M. G. Al-Shaal, M. Calin, I. Delidovich and R. Palkovits, *Catal. Commun.*, 2016, **75**, 65–68.
21 Z. P. Yan, L. Lin and S. Liu, *Energy Fuels*, 2009, **23**, 3853–3858.
22 A. M. Hengne, N. S. Biradar and C. V. Rode, *Catal. Lett.*, 2012, **142**, 779–787.
23 J. M. Nadgeri, N. Hiyoshi, A. Yamaguchi, O. Sato and M. Shirai, *Appl. Catal., A*, 2014, **470**, 215–220.
24 Y. Kuwahara, Y. Magatani and H. Yamashita, *Catal. Today*, 2015, **258**, 262–269.
25 N. L. Rosi, J. Eckert, M. Eddaoudi, D. T. Vodak, J. Kim, M. O'keeffe and O. M. Yaghi, *Science*, 2003, **300**, 1127–1129.
26 H. Furukawa, N. Ko, Y. B. Go, N. Aratani, S. B. Choi, E. Choi, A. Ö. Yazaydin, R. Q. Snurr, M. O'Keeffe and J. Kim, *Science*, 2010, **329**, 424–428.
27 K. Sumida, D. L. Rogow, J. A. Mason, T. M. McDonald, E. D. Bloch, Z. R. Herm, T. H. Bae and J. R. Long, *Chem. Rev.*, 2011, **112**, 724–781.
28 J. H. Cavka, S. Jakobsen, U. Olsbye, N. Guillou, C. Lamberti, S. Bordiga and K. P. Lillerud, *J. Am. Chem. Soc.*, 2008, **130**, 13850–13851.
29 M. Kandiah, M. H. Nilsen, S. Usseglio, S. Jakobsen, U. Olsbye, M. Tilset, C. Larabi, E. A. Quadrelli, F. Bonino and K. P. Lillerud, *Chem. Mater.*, 2010, **22**, 6632–6640.
30 M. J. Katz, Z. J. Brown, Y. J. Colón, P. W. Siu, K. A. Scheidt, R. Q. Snurr, J. T. Hupp and O. K. Farha, *Chem. Commun.*, 2013, **49**, 9449–9451.
31 G. Huang, Q. Yang, Q. Xu, S. H. Yu and H. L. Jiang, *Angew. Chem., Int. Ed.*, 2016, **128**, 7505–7509.
32 H. Liu, L. Chang, C. Bai, L. Chen, R. Luque and Y. Li, *Angew. Chem., Int. Ed.*, 2016, **55**, 5019–5023.
33 F. M. Zhang, S. Zheng, Q. Xiao, Y. J. Zhong, W. D. Zhu, A. Lin and M. S. El-Shall, *Green Chem.*, 2016, **18**, 2900–2908.
34 Z. Guo, C. Xiao, R. V. Maligal-Ganesh, L. Zhou, T. W. Goh, X. Li, D. Tesfagaber, A. Thiel and W. Huang, *ACS Catal.*, 2014, **4**, 1340–1348.
35 Y. M. Chung, H. Y. Kim and W. S. Ahn, *Catal. Lett.*, 2014, **144**, 817–824.
36 Y. Kuwahara, H. Kango and H. Yamashita, *ACS Sustainable Chem. Eng.*, 2017, **5**, 1141–1152.
37 J. Kim, S. N. Kim, H. G. Jang, G. Seo and W. S. Ahn, *Appl. Catal., A*, 2013, **453**, 175–180.
38 F. G. Cirujano, A. Corma and F. L. I. Xamena, *Catal. Today*, 2015, **257**, 213–220.
39 J. Hajek, M. Vandichel, B. Van de Voorde, B. Bueken, D. De Vos, M. Waroquier and V. Van Speybroeck, *J. Catal.*, 2015, **331**, 1–12.
40 M. L. Foo, S. Horike, T. Fukushima, Y. Hijikata, Y. Kubota, M. Takata and S. Kitagawa, *Dalton Trans.*, 2012, **41**, 13791–13794.
41 P. Küsgens, M. Rose, I. Senkovska, H. Fröde, A. Henschel, S. Siegle and S. Kaskel, *Microporous Mesoporous Mater.*, 2009, **120**, 325–330.
42 R. Fang, H. Liu, R. Luque and Y. Li, *Green Chem.*, 2015, **17**, 4183–4188.
43 Q. Yuan, D. Zhang, L. van Haandel, F. Ye, T. Xue, E. J. Hensen and Y. Guan, *J. Mol. Catal. A: Chem.*, 2015, **406**, 58–64.
44 F. Zhang, Y. Jin, Y. Fu, Y. Zhong, W. Zhu, A. A. Ibrahim and M. S. El-Shall, *J. Mater. Chem. A*, 2015, **3**, 17008–17015.
45 Z. Hu, Y. Peng, Y. Gao, Y. Qian, S. Ying, D. Yuan, S. Horike, N. Ogiwara, R. Babarao and Y. Wang, *Chem. Mater.*, 2016, **28**, 2659–2667.
46 G. Akiyama, R. Matsuda, H. Sato, M. Takata and S. Kitagawa, *Adv. Mater.*, 2011, **23**, 3294–3297.
47 M. G. Al-Shaal, W. R. H. Wright and R. Palkovits, *Green Chem.*, 2012, **14**, 1260–1263.

